ELSEVIER

Contents lists available at ScienceDirect

Review of Palaeobotany and Palynology

journal homepage: www.elsevier.com/locate/revpalbo



A millennium of anthropic and climate dynamics in the Lake Izabal Basin, eastern lowland Guatemala



Erdoo Mongol ^{a,*}, Francisca Oboh-Ikuenobe ^a, Jonathan Obrist-Farner ^a, J. Enrique Moreno ^b, Alex Correa-Metrio ^c

- ^a Missouri University of Science and Technology, Department of Geosciences and Geological and Petroleum Engineering, Rolla, MO 65409, USA
- ^b Center for Tropical Paleoecology and Anthropology, Smithsonian Tropical Research Institute, Panama
- ^c Centro de Geociencias, Universidad Nacional Autónoma de México, Santiago de Queretaro, 76230, Mexico

ARTICLE INFO

Article history: Received 17 November 2022 Received in revised form 16 February 2023 Accepted 22 February 2023 Available online 26 February 2023

Keywords: Lake Izabal Vegetation history Anthropogenic impacts Pollen analysis Elemental geochemistry

ABSTRACT

Modern precipitation gradients across the Maya region in Central America result in a diverse vegetational mosaic that varies from scrub forest to rainforest. In this region, evidence of past changes in the distribution of vegetation indicates two main patterns: i) a Holocene long-term trend towards a more seasonal forest, and ii) sharp changes in vegetation cover resulting from human occupation. The history of vegetation in moister areas of the Maya region, however, has been mostly extrapolated from studies carried out in the Yucatan Peninsula. We reconstructed the paleoenvironmental and paleoecological dynamics of the last ~1300 years in the Lake Izabal Basin, one of the wettest areas within the Maya region. Palynological and geochemical evidences indicate that from ~650-1150 CE, vegetation assemblages were dominated by disturbance taxa, under relatively low erosion in the catchment area. This pattern probably resulted from anthropogenic activities during the Terminal Classic Period (800-950 CE) combined with the dry and more seasonal conditions of the Medieval Climate Anomaly. The record from 1150 to 1400 CE points to an increase in moisture availability with a change towards a forested landscape. From 1400 to 1950 CE, geochemical data indicate lower precipitation, while the vegetation appears less fragmented and a mature forest developed. Such pattern probably emerged from lower evapotranspiration associated with the Little Ice Age (1350-1850 CE) favoring vegetation recovery. During the last 1300 years, vegetation change in the Lake Izabal Basin parallels that of the Yucatan Peninsula, with anthropogenic influences and moisture availability exerting first- and second-order controls on vegetation turnover, respectively.

© 2023 Elsevier B.V. All rights reserved.

1. Introduction

In the Neotropics, the late Holocene has been characterized by forest cover variability at millennial to centennial timescales caused by climatic and/or anthropogenic changes (e.g. Leyden, 2002; Beach et al., 2009; Correa-Metrio et al., 2012a,b, 2013, 2016; Caballero-Rodríguez et al., 2017, 2018; Harvey et al., 2019; Bush et al., 2021). Regional climatic changes have been associated with the dynamics of the Intertropical Convergence Zone (ITCZ), the El Niño Southern Oscillation (ENSO) system, the North Atlantic Oscillation (NAO), the structure of sea surface temperatures (SST) in the Caribbean Sea, among others (e.g. Hodell et al., 2005a; Mann et al., 2009; Correa-Metrio et al., 2014a; Bhattacharya et al., 2017). The confluence of these different factors, combined with anthropogenic disturbance, has resulted in changes in vegetation composition and structure as plants are preferentially

aligned according to their adaptability potential and/or tolerance to environmental conditions (Correa-Metrio et al., 2013; Delcourt and Delcourt, 1991).

The Yucatan Peninsula and adjacent mountain systems, hereafter referred to as the Maya Region (Fig. 1), are characterized by a high biodiversity that results from the conjunction of Neotropical and Nearctic biotas interacting across steep environmental gradients (Graham, 2010a; Correa-Metrio et al., 2011). The distribution of vegetation types across the region, which ranges from scrub forest in the north to tropical rain forest in the south, is driven by the regional precipitation gradient characterized by dry conditions in the northern areas and prevailing wet conditions in the south along mountain ranges (Fig. 1C) (White and Hood, 2004; Rzedowski, 2006). These ecosystems have undergone diverse degrees of degradation in the past, because of either climatic or human influence. Numerous palynological studies have reported a temporal pattern of vegetation community change consisting of a gradual increase in disturbance taxa throughout the Holocene (e.g., Islebe et al., 1996; Leyden, 2002; Mueller et al., 2009), largely

^{*} Corresponding author. E-mail address: emzcb@mst.edu (E. Mongol).

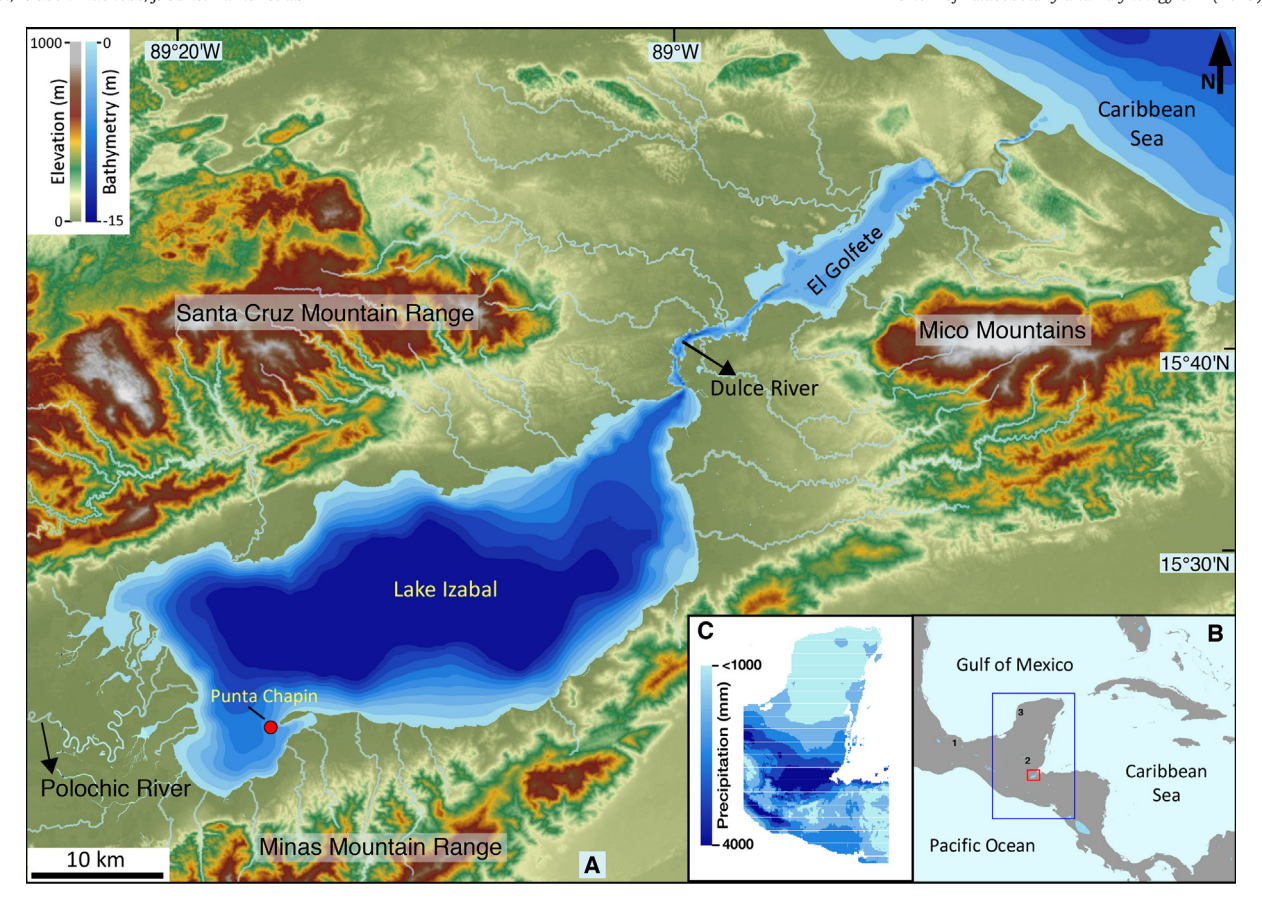


Fig. 1. A. Lake Izabal in the regional topographic context with the bathymetric outline of the lake; the red dot shows the location of the Punta Chapin sediment core (modified from Obrist-Farner et al., 2022a). B. Location of Lake Izabal in the context of Central America (red rectangle), with the blue rectangle highlighting the area associated with the Maya Region. Numbers 1–3 showing location of Lago Verde, Oquevix and Aguada X'Caamal respectively. C. Mean annual precipitation across the Maya Region (blue rectangle in inset B between 14–22°N and 84–94°W) (precipitation data from USGS Google Earth Engine). (For interpretation of the references to color in this figure legend, the reader is referred to the web version of this article.)

attributed to the progressive southward migration of the ITCZ that has resulted in drier conditions in the Northern Hemisphere (Curtis et al., 1996; Beach et al., 2009; Caffrey et al., 2011; Nooren et al., 2018). Superimposed on this long term trend is evidence of substantial changes in forest cover during the late Holocene associated with human activities and deforestation (Islebe et al., 1996; Brenner et al., 2002, 2003; Beach et al., 2009; Franco-Gaviria et al., 2018b). While disentangling anthropic and climatic signals is difficult, it is paramount for a better understanding of the interaction between these two sources of ecosystem variability, especially under the modern scenario of global change and pervasive human occupation.

While vegetation turnover in the Yucatan Peninsula has been rather well studied, relatively little is known about the evolutionary history of ecosystems in the areas of higher precipitation within the Maya region, such as the Lake Izabal Basin (LIB) in eastern Guatemala (Fig. 1C). The LIB, located in the eastern part of the southern Maya lowlands, has a mean annual precipitation between 3000 and 4000 mm/yr, which is significantly higher when compared to other areas within the Maya Region (Fig. 1C). The higher rainfall in the LIB results from orographic precipitation of moisture carried from the Caribbean Sea by the regional trade winds (Martinez et al., 2019). Changes in the oceanic and atmospheric circulation patterns in the region have resulted in variability of the regional climate (Duarte et al., 2021). Thus, factors such as the Caribbean Low Level Jet and the Atlantic Warm Pool have played a role at modulating the history of the regional climate (Duarte et al., 2021) and the regional ecosystems. Given the moister conditions in the LIB area, the basin could have buffered adverse effects of extreme climatic conditions

in the regional ecosystems by providing ecological refugia, thus supporting the resilience of regional forests (Correa-Metrio et al., 2014a; Rull, 2009).

The Punta Chapin core, retrieved from Lake Izabal (Fig. 1), is a 1300year-long sedimentary record (Hernández et al., 2020) that provides the opportunity for palynological and geochemical analyses to study the vegetation and environmental dynamics in the area. Qualitative and quantitative analyses of palynomorphs (pollen, spores, algae) and X-ray fluorescence (XRF) of elemental abundances have been undertaken to reconstruct vegetation changes and environmental dynamics through time. The record provides an opportunity to compare the environmental dynamics of the LIB with other records from the Maya Region in the context of the Medieval Warm Period and the Little Ice Age, the most important climatic oscillations of the last two millennia (Mann et al., 2009; McGregor et al., 2015; Anchukaitis and Smerdon, 2022.), and the pervasive occupation and posterior disintegration of the Maya civilization (Leyden, 2002). Using a high-resolution geochemical record and a ~100-year-resolution pollen sequence, we offer an overview of environmental and ecological dynamics in the LIB during the last ~1300 years. This reconstruction provides the means for evaluating the role that the regionally disjointed climate might have played at modulating vegetation dynamics during the last ~1300 years.

2. Study area

Lake Izabal is located in eastern Guatemala, in the Maya lowlands, between latitudes 15° 24'N – 15° 38'N and longitudes 88° 58'W – 89°

25'W along the Polochic-Motagua Fault System (Fig. 1; Bartole et al., 2019; Obrist-Farner et al., 2020). The lake is shallow ($z_{max} = 15 \text{ m}$), with the water surface at ~1.5 m above mean sea level (Hernández et al., 2020; Duarte et al., 2021). With a surface area of 672 km², Lake Izabal is the largest lake in Guatemala and the third largest in the northern Neotropics (Brinson and Nordlie, 1975; Obrist-Farner et al., 2019). Flanked by the Santa Cruz Mountain Range to the north and the Minas Mountain Range to the south, the lake has a large catchment basin that is fed predominantly by the Polochic River (Fig. 1). The Dulce River, on the other hand, constitutes the main outflow channel that drains into the Caribbean Sea (Brinson and Nordlie, 1975; Obrist-Farner et al., 2019). Regional precipitation is seasonal, in tandem with the intra-annual latitudinal migration of the Intertropical Convergence Zone (ITCZ) (Duarte et al., 2021). The region has a high mean annual precipitation (~3300 mm/year), which is about two times higher than that of the Peten region and environs (~1800 mm/year) and other places in the Maya region (Duarte et al., 2021). The rainy season lasts from May to November, with a slight decrease in precipitation during the mid-summer drought caused by strengthening of the Caribbean Low-Level Jet (Magaña et al., 1999).

The regional geology is composed of metamorphosed serpentinite, gneiss, and schist, and sedimentary sequences towards the Santa Cruz Mountain Range in the NW and the Minas Mountain Range in the south, (Wilson, 1974; Giunta et al., 2002). To the east, the Mico Mountains (Fig. 1) are composed of Cretaceous metamorphic and Miocene siliciclastic rocks (Vinson, 1962; Obrist-Farner et al., 2020).

Besides the abundant rainfall that typifies the LIB, the region is warm, constituting a tropical lowland environment, characterized by dense vegetation (Standley and Steyermark, 1945). Regional vegetation cover is part of the multifaceted and highly diversified flora of Guatemala, which is the richest and most diversified in Central America (Standley and Steyermark, 1945; Steyermark, 1950). Such high biodiversity results from the convergence of species from the Nearctic and Neotropical biogeographic realms interacting along the steep environmental gradients that mostly result from regional both climates and topography (Standley and Steyermark, 1945; Steyermark, 1950; Graham, 2010b). The lowland areas with welldrained soil are mostly occupied by tropical evergreen to semievergreen closed canopy forests and dominated by taxa belonging to families such as Fabaceae, Anarcadiaceae, Arecaceae, Sapindaceae, Meliaceae, Betulaceae, Euphorbiaceae, Bignoniaceae, Malvaceae, Pinaceae, as well as herbaceous families such as Poaceae, Asteraceae, and Amaranthaceae (Standley and Stevermark, 1945; Stevermark, 1950; Islebe and Hooghiemstra, 1995; Islebe et al., 1996; Graham, 2010a). In the eastern lowlands, marshes and riparian mangroves dominated by aquatic vegetation (e.g., *Rhizophora* spp.) are abundant, especially along the shores and floodplains of the lake (Standley and Steyermark, 1945; Steyermark, 1950).

3. Materials and methods

In 2017, a 455 cm-long core was collected under a water column of 5 m in Punta Chapin, southwestern side of Lake Izabal (Fig. 1). The uppermost 55 cm were collected using a mud-water interface (MWI) corer (Fisher et al., 1992), extruded, sectioned at 3-cm intervals, packed and stored in coolers. Consolidated sediment sections were collected utilizing the modified Livingstone corer (Deevey, 1965) for a total depth of 455 cm. The sections were kept inside polycarbonate core barrels, sealed, labeled, and shipped to Missouri University of Science and Technology for further analyses.

Eight samples of terrestrial organic matter (woody debris and charcoal fragments) were collected from the consolidated core sections for radiocarbon dating (See Table 1). The samples were washed with deionized water on a 63-µm sieve, dried, and submitted to the National Ocean Sciences Accelerator Mass Spectrometer (NOSAMS) facility at Woods Hole Oceanographic Institution for radiocarbon dating. A Bayesian age-depth model was constructed using the *rbacon* package in R (Blaauw and Christen, 2011; Fig. 2), which calibrates radiocarbon dates using the IntCal20 curve (Reimer, 2020). The age-depth model was further constrained using the date of core collection (i.e., 2017 CE).

Twelve samples spread throughout the core at 33 cm intervals were processed for palynological analysis. Five grams of each sample were processed at Global Geolab Limited in Alberta, Canada, using the standard technique of digesting sediments in hydrochloric acids, hydrofluoric acids, and acetolysis (Faegri et al., 1989) and strew mounting the organic residues on permanent glass slides for analysis. Pollen morphotypes were identified at the finest possible taxonomic level using the palynological collection at the Smithsonian Tropical Research Institute (STRI), Panama (Moreno et al., 2014), the literature (Roubik and Moreno, 1991; Colinvaux et al., 1999; Jaramillo and Dilcher, 2001; Punt et al., 2007), and electronic resources (Bush and Weng, 2007; Jaramillo and Rueda, 2019; Tropicos of the Missouri Botanical Garden, 2020). Pollen observations and counting were carried out under a Nikon Eclipse 80i transmitted light microscope, and photomicrographed at 400× and 1000× magnifications using a Nikon Digital Camera DXM 1200f and NIS (Nikon Imaging Software) -Elements D.5.11.00 64-bit. The identified pollen grains were categorized according to ecological preferences into herbaceous, closed-canopy forests, conifers and temperate taxa (Fig. 3; Supplementary Table 1). The pollen sum (sampling effort) was set up at 300 pollen grains, excluding

Table 1AMS ¹⁴C dates from the Punta Chapin core, sample type used for ¹⁴C dating and its stratigraphic position along the core. Calibrated ages according to IntCal20 (Reimer, 2020), and modeled ages according to the Bayesian age-depth model constructed using Bacon (Blaauw and Christen, 2011).

Depth (cm)	Sample type	14C age \pm error	Calibrated age (CE) Probabilities in parenthesis	Modeled date (CE) (95% ranges in parenthesis)
0	Date of core collection		2017	2017 (2014–2020)
58.5	Charcoal	150 ± 60	1794–1950 (0.53) 1664–1785 (0.42)	1910 (1859–1950)
			1906–1944 (0.19) 1833–1891 (0.27)	
108	Wood fragment	145 ± 20	1798–1821 (0.10) 1720–1779 (0.24)	1819 (1751–1873)
120.5	Charcoal	280 ± 70	1671–1709 (0.15) 1424–1459 (0.95)	1796 (1724–1852)
214	Wood fragment	235 ± 15	1644–1667 (0.60); 1796–1782 (0.35)	1631 (1527–1665)
304	Wood fragment	450 ± 15	1424–1459 (0.95)	1420 (1303-1457)
368	Wood fragment	815 ± 15	1219-1265 (0.95)	1187 (1053–1257)
404	Charcoal	1160 ± 70	762–1019 (0.86); 686–742 (0.09)	954 (855–1043)
445	Wood fragment	1230 ± 15	786–877 (0.76); 706–738 (0.19)	729 (678–822)

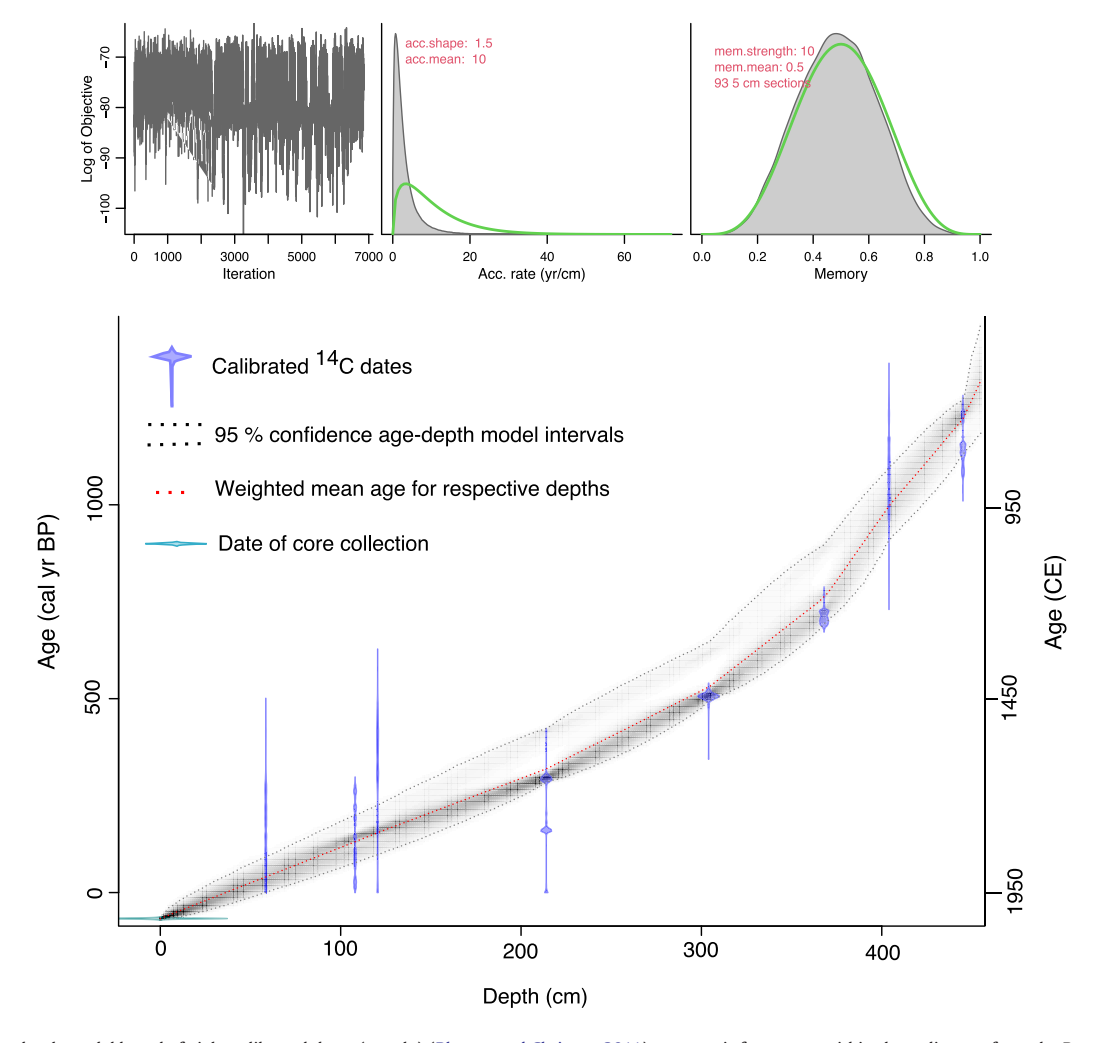


Fig. 2. Bayesian age-depth model based of eight calibrated dates (purple) (Blaauw and Christen, 2011) on organic fragments within the sediments from the Punta Chapin core. (For interpretation of the references to color in this figure legend, the reader is referred to the web version of this article.)

Cyperaceae, *Rhizophora*, *Quercus* and conifers, which were nevertheless counted (after Correa-Metrio et al., 2011). Abundances of all taxa were transformed to percentages of the pollen sum in each sample.

For pollen identification, we followed the methods of Holst et al. (2007) and Whitney et al. (2012) and assigned Poaceae pollen types (monoporate) with sizes > 80 µm and smooth ornamentation to Zea mays (domesticated maize) in comparison with the smaller-sized and ornamented wild counterpart Zea sp. (teosinte). Amaranthus and Chenopodium pollen types could not be distinguished because of their close resemblance and similar morphological attributes. In addition, Pinus and Podocarpus were grouped together as conifers because their abundances and distribution patterns were similar. The pollen dataset was summarized using a detrended correspondence analysis (DCA) (Correa-Metrio et al., 2014b).

Density and magnetic susceptibility (MS) were measured on the consolidated sediment cores before core splitting using a GeoTek multi-sensor core logger at the University of Florida. The cores were then sectioned lengthwise and imaged using a line-scan camera on the GeoTek logger. X-ray Fluorescence (XRF) core scanning was carried out at the Large Lakes Observatory, University of Minnesota-Duluth. Core surfaces were cleaned, smoothed, and then scanned by the ITRAX XRF core scanner using a Cr source tube at 30 kV and 55 mA, at 5-mm resolution with a 15 s dwell time. The mud-water-interface (MWI) samples were homogenized, placed in plastic containers, and scanned at 1-mm resolution to obtain ~20 measurements per sample with a

15 s dwell time. The XRF comprised forty-two elements in total, but only eight elements that showed significant variability were used for the environmental interpretation. The geochemical dataset was standardized and analyzed using a principal components analysis (PCA) to assess the temporal variability of the record and the relationships among elements (Jolliffe, 1986).

The pollen diagram and all statistical analyses were performed in R (R Core Team, 2021), using packages *rioja* (Juggins, 2017) and vegan (Oksanen et al., 2020).

4. Results

4.1. Core description and chronology

The Punta Chapin core was characterized by homogeneous gray mud, with sparse laminae and very thin beds of silt and sand. Organic debris were minimal in the core. All radiocarbon dates were in stratigraphic order and the resulting age-depth model suggests that the core covers the last ~1300 years, with sedimentation rates increasing towards the present (Fig. 2).

4.2. Palynology and geochemistry

Palynomorph recovery was high with well-preserved morphological attributes throughout the Punta Chapin core. The palynomorphs were

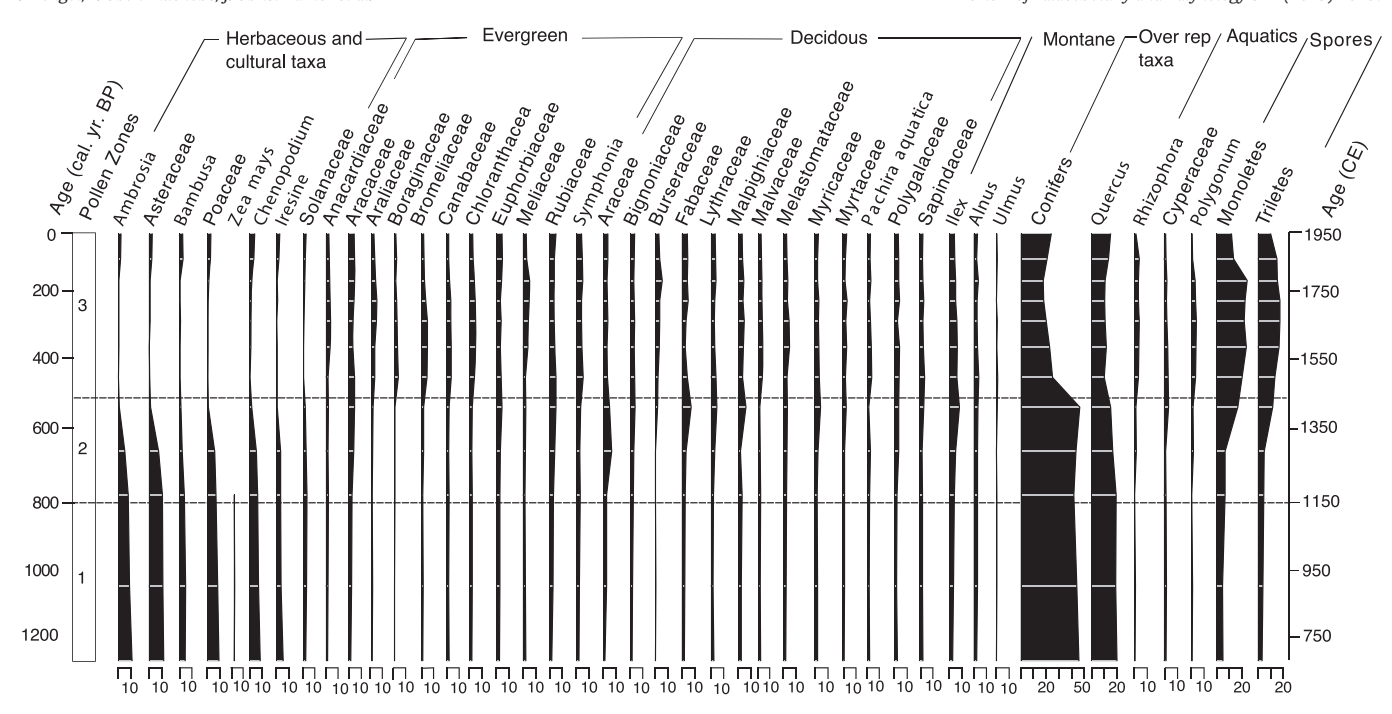


Fig. 3. Relative abundances of selected taxa of the Punta Chapin sedimentary record. Percentages were calculated based on the pollen sum of each sample.

classified into 67 pollen morphotypes, eight spore types, two nonmarine algal types, and various types of fungal remains (Fig. 3, Supplementary Table 1). Angiosperms dominated the pollen assemblage, whereas only two taxa were identified among the abundant and overrepresented gymnosperms (*Pinus* and *Podocarpus*). Unidentified pollen grains represented less than 10% of the total pollen count in each sample (Supplementary Table 1). The general pattern of change was characterized by an increase of tropical forest taxa at ~1350 CE at the expense of herbaceous and cultural taxa (Fig. 3).

In the DCA ordination, herbaceous pollen taxa probably associated with disturbance (*Ambrosia*, Asteraceae, *Amaranthus/Chenopodium*, Poaceae, *Bambusa* and *Zea mays*) (Marchant et al., 2002; Franco-

Gaviria et al., 2018a) were ordinated towards the positive side of DCA Axis 1, with scores ranging from 0.7 to 3.0 SD (standard deviations; Fig. 4A). Pollen taxa representative of forest cover (e.g., Fabaceae, Bignoniaceae, Malvaceae, Burseraceae, Arecaceae, Canabaceae) were, on the other hand, mostly ordinated towards the negative end of DCA Axis 1, with scores ranging from —2.0 to 0.2 SD (Fig. 4A). Along DCA Axis 2, evergreen forest taxa (e.g., Anacardiaceae, Bromeliaceae, Chloranthaceae, and Araliaceae, affinities after Correa-Metrio et al., 2011 and Marchant et al., 2002) mostly clustered towards the positive side, with scores ranging from 0.1 to 2.5 SD, while deciduous forest taxa (e.g., *Pachira aquatica*, Fabaceae, and Bignoniaceae, affinities after Correa-Metrio et al., 2011 and Marchant et al., 2002) mostly cluster

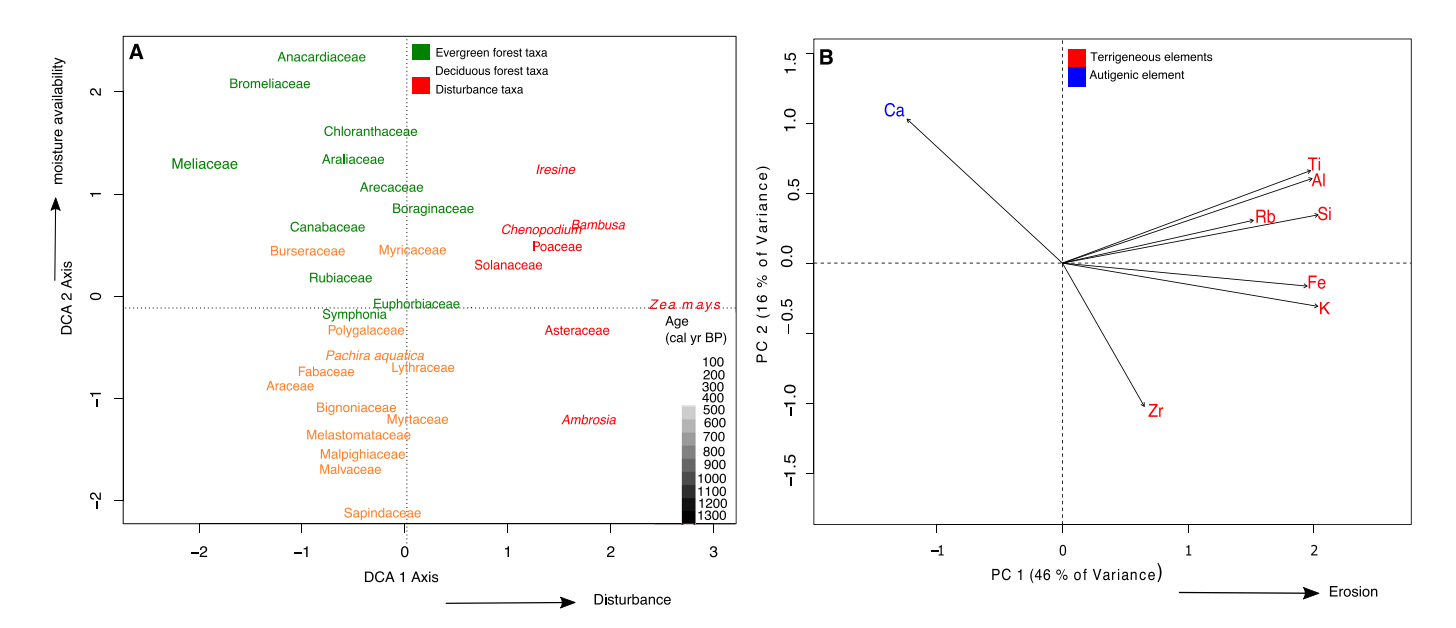


Fig. 4. Ordinations of the palynological and geochemical records of the Punta Chapin sedimentary record, lowland Guatemala. (A) DCA plot of palynological data showing selected pollen taxa. (B) PCA plot of selected elements in the Punta Chapin core. The terrigenous elements plot on the positive end of Axis 1 in red, which is authigenic, plots on the negative end of Axis 1 or positive end of Axis 2 in blue. (For interpretation of the references to color in this figure legend, the reader is referred to the web version of this article.)

towards the negative side, with scores ranging from -0.1 to -2.1 (Fig. 4A). Thus, whereas DCA Axis 1 provides a direct indication of the dominance of open vegetation (i.e., positive scores reflect open vegetation, while negative scores represent closed canopy forest), DCA 2 shows a gradient from deciduous to evergreen forest elements.

The geochemical record was characterized by eight elements (Titanium [Ti], Iron [Fe], Silicon [Si], Aluminum [Al], Rubidium [Rb], Potassium [K], Zircon [Zr], and Calcium [Ca]) that were selected for analysis because their abundances exhibited significant variability through time (Fig. 5), and they have been commonly used for reconstructing environmental conditions in lake sediments (e.g., Meyers, 1997, 2003; Boyle, 2002; Kylander et al., 2011; Franco-Gaviria et al., 2018b; Duarte et al., 2021). Al, Si, Ti, Rb, Fe, and K showed a similar trend of decreasing abundances from the bottom of the record to ~1150 CE, an increase between 1150 and 1400 CE and then a decreasing trend from 1400 CE to the present (Fig. 5). On the other hand, Zr showed variable abundances with a marked trend towards higher values from 1750 CE to present, while Ca abundance increased throughout the record (Fig. 5).

The first two principal components of the PCA performed on the geochemical dataset accounted for 62% of the variability, with PC1 and PC2 comprising 46% and 16% of the total variance, respectively (Fig. 4B). Terrigenic elements such as Ti, Al, Si, Fe, K, Si, and Rb were all positively correlated among them and aligned with PC1. Five of the terrigenic elements (Ti, Al, Si, Fe and K) ordinated the highest scores (\sim 2.0) along PCA Axis 1, while Rb and Zr record + 1.5 and + 0.8, respectively (Fig. 4B). Zr, with the lowest PCA Axis 1 score, had the lowest association with the other terrigenic elements. Conversely, Ca was ordinated towards the negative side of PC1 (-1.1) and a relatively high score for PC2 (+1.2), showing negative correlations with the rest of the dataset. The ordination of terrigenic elements to the positive side of PC1 suggest increased runoff to the lake, likely indicating fluctuations in terrigenous sediment input into the basin (Kylander et al., 2011; Duarte et al., 2021). The association of negative scores with Ca indicates this end of the axis reflects authigenic precipitation of carbonates. This dichotomy probably reflects changes in the rainfall/evaporation balance, which would translate into increased erosion during times of higher rainfall and increased precipitation of carbonates during times of higher evaporation (e.g., Mueller et al., 2009). Carbonate rocks present in the northeastern part of the basin are probably an important source of Ca into Lake Izabal as they could be drained by fluvial system into the lake or as a result of marine incursions (Obrist-Farner et al., 2022b). However, the coupling of the Ca/Ti ratio with the Ca abundance in the PC record (Fig. 5B) suggests that Ca input into the lake has been dominated by authigenic sources within the studied time interval. On the other hand, PC2 only displayed a clear association with Zr and Ca and, given the little associated variance (16%), we did not make an explicit interpretation of the axis.

Based on the changes in relative pollen percentages, elemental geochemistry data, and ordination scores (DCA and PCA), we subdivided the core into three main zones that illustrate the evolution of vegetation and environmental changes in the Lake Izabal region during the last 1300 cal yr BP (Fig. 3). Although we focused on the pollen data for analysis of vegetation dynamics of the region, the elemental geochemistry data supported our interpretation. The distinction was not a formal stratigraphic scheme, but rather was created to simplify the illustration and interpretation of the paleoenvironmental and paleoecological history of the area. The resultant pollen diagram shows stratigraphic changes in the respective vegetation groups, and the zones are interpreted as vegetational changes through time based on the observed pollen assemblages and their variations in time (Fig. 3; Supplementary Table 1).

4.2.1. Pollen Zone I (455-370 cm; 650-1150 CE)

This zone was characterized by high relative abundances of grass pollen (Poaceae) and pollen of Asteraceae, Amaranthaceae/Chenopodiaceae, and Solanaceae, which are characteristic of vegetation under intense disturbance regimes (Marchant et al., 2002; Franco-Gaviria et al., 2018a). *Zea mays* was recorded in this zone at 433 cm and 400 cm, corresponding to 722–894 and 875–1079 CE, respectively. Pollen grains of *Quercus* and conifers displayed high percentages in this zone, whereas taxa associated with closed-canopy forest and aquatic vegetation, and fern spores were low and poorly represented (Fig. 3). DCA Axes 1 and 2 sample scores were large and stable (Fig. 6 F and G). The elemental geochemistry was characterized by a decreasing trend in the abundances of Ti, Fe, Si, Al, Rb, K and Zr and a relative increase in Ca from 650 to 1150 CE (Fig. 4). Accordingly, PC1 sample scores were characterized by a decreasing trend along the zone (Fig. 6H).

4.2.2. Pollen Zone II (350-300 cm; 1150-1400 CE)

This zone was characterized by a decrease in pollen of herbaceous taxa, while pollen of closed-canopy forest families increased (Fig. 3). Pollen of herbaceous taxa/families, such as *Bambusa*, Asteraceae, *Ambrosia*, *Chenopodium* and *Iresine*, decreased sharply compared with

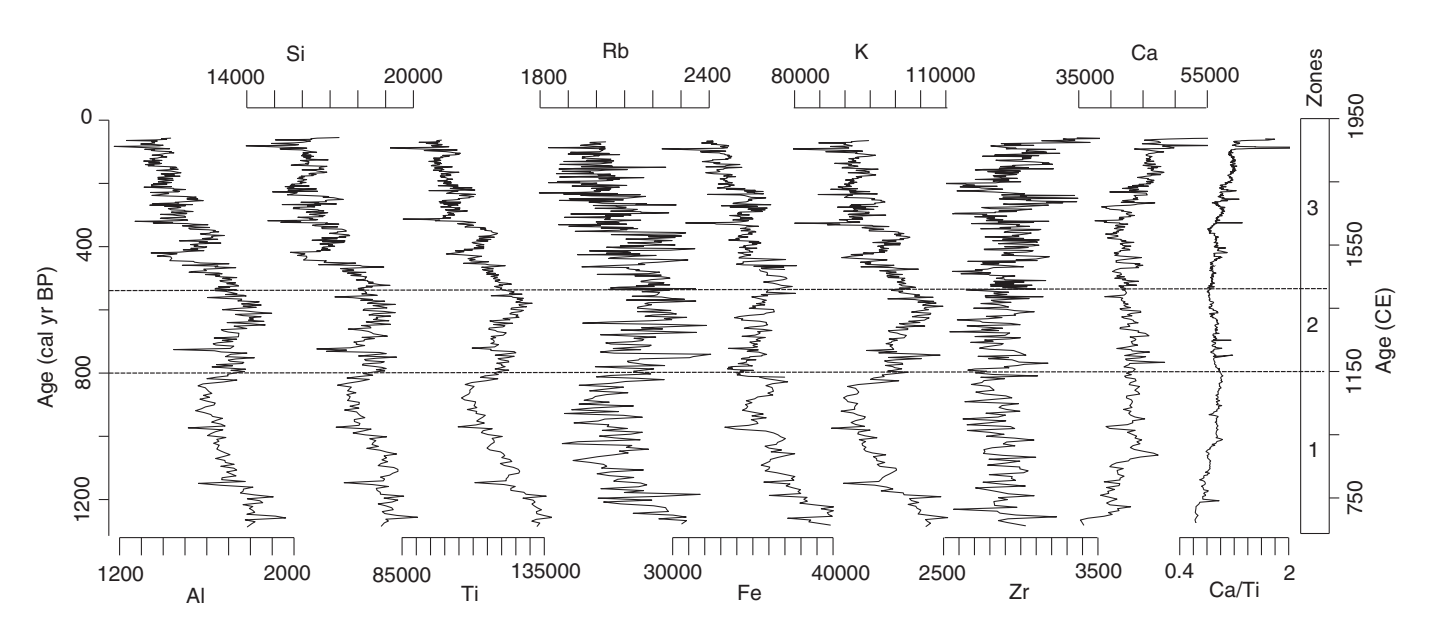


Fig. 5. Selected elements of the geochemical record of the Punta Chapin core.

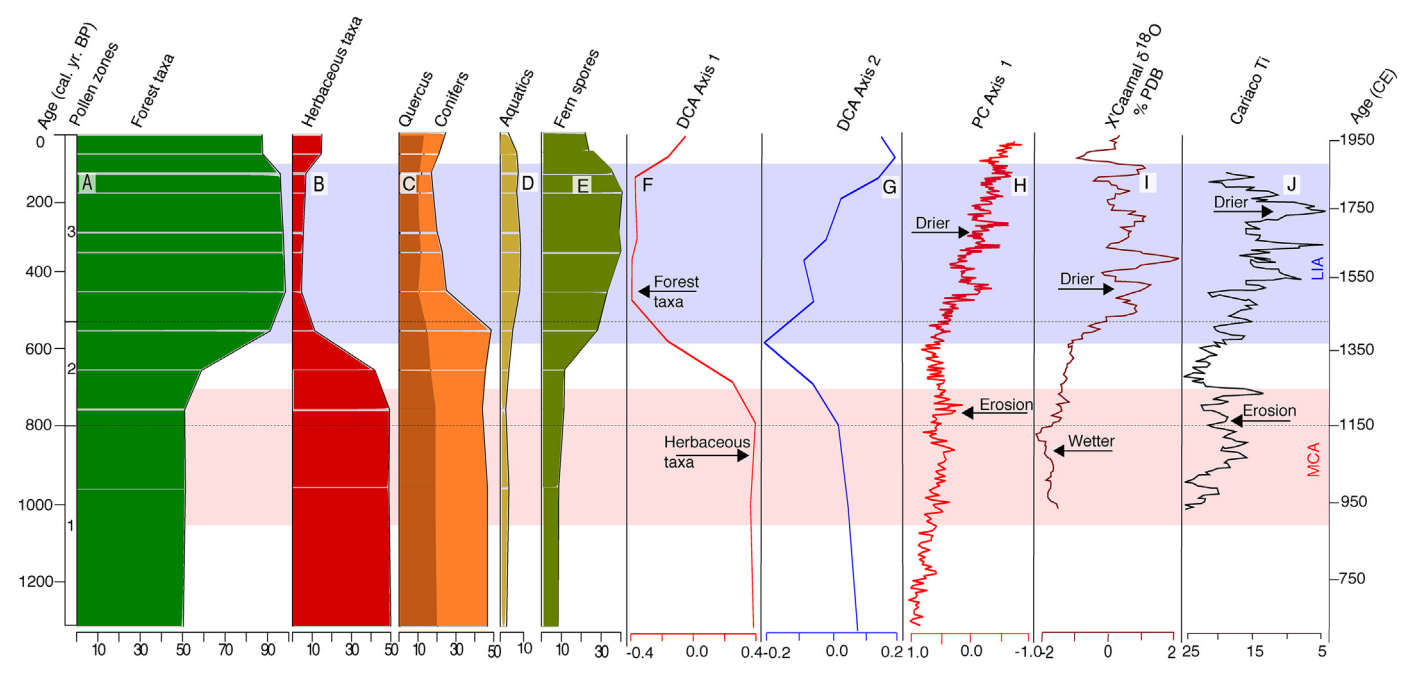


Fig. 6. Environmental and vegetation variability in the Lake Izabal Basin during the last ~1300 years. (A) Forest taxa. (B) Herbaceous taxa. (C) Quercus and Conifers. (D) Aquatics (E) Fern spores. (F) DCA Axis 1 time series plot. (G) DCA Axis 2 time series plot. (H) PCA Axis 1 time series plot. (I) Aguada X'caamal δ¹⁸O %PDB (Hodell et al., 2005a). (J) Cariaco Ti (Haug et al., 2001 in Hodell et al., 2005a). Note how the abundances of conifers and Quercus mimic those of the disturbance taxa that dominated the record from 650 to 1150 CE. Note scale differences on the x-axis

the gradual decrease of the pollen of Poaceae and Solanaceae. Pollen of Arecaceae, Boraginaceae, Meliaceae, and Sapindaceae appeared for the first time and gradually increased towards the upper part of the zone. Pollen grains of conifers were abundant, while those of aquatics and spores increased slightly. DCA Axis 1 sample scores showed a large and rapid transition from positive to negative values, whereas DCA Axis 2 scores were characterized by a large dip into negative scores (Fig. 6F and G). The elemental geochemistry data equivalent to this zone was characterized by an increasing abundance of Ti, Fe, Si, Al, Rb, K and Zr and a relative decrease of Ca (Fig. 5) that reflected on higher and relatively stable values of PC1 (Fig. 6H).

4.2.3. Pollen Zone III (300-66 cm; 1400-1950 CE)

Pollen grains of herbs all together made up to ~7% of the pollen sum. While pollen grains of the Bromeliaceae and Anacardiaceae families appeared in this zone for the first time, pollen grains belonging to various closed-canopy forest taxa increased in relative abundance, reaching ~93%. The relative abundances of the aquatics and fern spores notably increased in this zone (Fig. 3). Whereas DCA Axis 1 sample scores were characterized by stable negative values, Axis 2 showed a trend towards positive values (Figs. 5A, 6F and G). The geochemistry of the sediments in this zone was characterized by gradually decreasing abundances of Ti, Fe, Si, Al, Rb, K, and Zr, and increasing concentrations of Ca (Fig. 5). These patterns of sediment composition were summarized by a substantial trend towards more positive values for the terrigenous elements and negative value for Ca in PC1 time series plot (Fig. 6H). From 1850 CE to present, disturbance taxa and conifers increased their abundances, coinciding with a relative decrease in some of the forest taxa, aquatics and fern spores (Figs. 3, 6A, B and C).

5. Discussion

The Punta Chapin core offers evidence into the evolution of the regional vegetation during the last 1300 years. Overall, vegetation turnover has been characterized by a progressive replacement of open and disturbed vegetation by closed canopy forests, which, according to the

geochemical record, have been closely associated with the erosive regimes of the area. Whereas abundances of herbaceous taxa provide a direct indication of the dominance of highly disturbed vegetation (either by climatic or anthropic agents), abundances of forest taxa indicate the development of a dense vegetation cover. Although conifers and Quercus are important components of montane forests in the Nearctic-Neotropical transition zone (Nixon, 2006; Richardson, 1998), in the LIB, they are likely associated with disturbance since they behave as opportunistic taxa under moist, warm conditions, (Correa-Metrio et al., 2011; Franco-Gaviria et al., 2018a). Indeed, in the Punta Chapin sediments core sediments, abundances of Quercus and conifers closely correlate with those of disturbance taxa (Figs. 3 and 6). Aquatic taxa (i.e. Cyperaceae, Rhizophora, and Polygonum) and fern spores in the PC record, in contrast, represent marshlands and riparian mangroves that develop along river floodplains (Standley and Steyermark, 1945). The correlation of their abundances with forest expansion (Fig. 6D) is probably associated with anthropogenic disturbance patterns. During times of pervasive human occupation, marshlands and riparian mangroves were transformed into agricultural farmlands that recovered after abandonment (Guderjan and Krause, 2011; Krause et al., 2021; Leonard et al., 2019).

Pollen Zone I (650–1150 CE) was characterized by high percentages of disturbance taxa (grasses and weeds; Figs. 3, 6B), including the pollen of *Zea mays* encountered at 650–700 CE and 950–1000 CE, which reflect on the high DCA Axis 1 scores (Fig. 5A, 6F). These findings indicate anthropogenic activities in close proximity to the lake, coinciding with the Maya Terminal Classic Period (TCP, from ~800 to 950 CE), which was a time interval characterized by large-scale deforestation linked to agricultural practices in the Maya region (e.g., Leyden, 1987, 2002; Islebe et al., 1996; Mueller et al., 2009, 2010; Turner and Sabloff, 2012; Wahl et al., 2007a, 2007b, 2016) and generally dry conditions (e.g., Hodell et al., 1995; Curtis et al., 1996; Medina-Elizalde et al., 2010). The relatively high abundances of *Quercus* and conifers in this zone (Figs. 3, 6C) as opposed to other forest taxa supports our interpretation of intensified local disturbance in the area, although these could also be indicating secondary forest regrowth at higher elevations

(Franco-Gaviria et al., 2018b; Harvey et al., 2019). The bottom of this zone was characterized by the high abundance of terrigenic elements and lowest abundance of Ca, indicating high erosion probably caused by the Maya land clearance. Erosion, however, decreased through the zone as indicated by decreasing scores of PC1 time series plot through Zone 1(Fig. 6H), reflecting a progressive reduction of precipitation (Boyle, 2002; Kylander et al., 2011; Duarte et al., 2021) due to drier conditions during the TCP and/or erosion control practices by the Maya that were common across riparian floodplains (Krause et al., 2021).

Although forest clearance and land disturbance can result in increased erosion (Dull, 2007), our results suggest that precipitation was the dominant factor influencing the mobilization of terrigenic elements into the lake during Pollen Zone I. This pollen zone also partly overlaps with the Medieval Climate Anomaly (MCA), which lasted from 950 to 1250 CE (Mann et al., 2009). The period prior to and during parts of the MCA was the driest in the last 1000 years based on syntheses of available regional proxy records across the northern Neotropics (Bhattacharya et al., 2017). Thus, while anthropogenic activities may have favored the prevalence of disturbance-associated vegetation at the expense of forested areas, dry conditions during the MCA likely undermined the proliferation of forest vegetation (Fig. 6).

Pollen Zone II, spanning from 1150 to 1400 CE, was characterized by a systematic reduction in the abundance of disturbance taxa and a surge in the abundance of forest and wetland taxa (Fig. 3). The abundances of terrigenic elements indicate a change from decreasing to increasing erosion, probably because of a moisture rebound. This process started ~200 years after the Mayan collapse in the Yucatan Peninsula, which occurred around 950 CE (Hodell et al., 1995). Thus, it is possible that increasing forest and swamp cover was associated with higher moisture availability. Furthermore, slight decrease in the abundance of Ca during this time (Fig. 5) signifies lower evaporation and increase precipitation (E/P) values in response to surplus moisture budget in the area arising from increased precipitation. PC1 scores slightly increased through the zone on the time series plot (Fig. 6H), probably indicating a period of increased catchment erosion caused by higher rainfall. Our inference of an increase in precipitation is supported by pollen data, with DCA Axis 2 indicating a surge in the representation of deciduous forest taxa (Figs. 5A, 6G), likely favored at the early successional stages of forest recovery indicated by the pollen data.

Pollen Zone III, spanning from 1400 to 1950 CE, was marked by a substantial increase in forest taxa and a decrease in disturbance taxa (Fig. 3), indicating a substantial expansion of dense canopy forests in the region. This pattern is summarized by the DCA ordination, with Axis 1 time series plot showing low scores that represent closed canopy forests, and Axis 2 displaying the largest scores throughout the record, implying a dominance of evergreen vegetation elements (Figs. 5A, 6F and G). This expansion correlates with a gradual reduction in the abundance of terrigenic elements, suggesting a long-term reduction in erosion. Similarly, increasing abundance of Ca (Fig. 4) points to long term relatively higher E/P that correlates with the hemispheric trend towards drier conditions (Haug et al., 2001). This reduction in precipitation is also observed in a nearby speleothem record from southern Belize (Kennett et al., 2012), suggesting decreased precipitation during forest recovery. Forest recovery was probably a result of lower anthropic pressure and that decreased erosion could have resulted from both decreasing rainfall and increased forest cover in the catchment.

In the Yucatan Peninsula, the conditions during the Little Ice Age (LIA, from 1300 to 1850 CE, Mann et al., 2009) have been reported as drier (Hodell et al., 2005b) but precipitation trends across western Central America during this time appear to have been variable (Steinman et al., 2022). The conditions in the LIB and southern Belize appear to have been wetter during the onset of the LIA, with precipitation progressively decreasing from ~1400 CE to the present (Obrist-Farner et al., 2022a). This is supported by our geochemical data and coincides with the period of the onset of forest recovery during Pollen Zone II. From ~1400 CE to the present, lower evapotranspiration rates associated

with the lower temperatures that characterized this climatic period (Mann et al., 2009) probably compensated the decrease in moisture availability in the LIB region. Thus, this relatively low moisture deficit created favorable conditions for a closed-canopy forest in the Lake Izabal region, similar to those reported for other locations in Central America and Mexico (Leyden, 2002; Lozano-García et al., 2007; Wahl et al., 2007a; Correa-Metrio et al., 2016). The forest recovery might have also contributed to the lower abundance of terrigenic elements because vegetation cover prevented erosion and mobilization of sediments into the lake. In addition, given the presently wetter conditions of the LIB compared with other locations in the Maya region (blue rectangle, Fig. 1B), precipitation reduction was probably not as severe to the vegetation relative to the other locations in Central America. Also, the time span of maximum forest expansion in this zone overlaps with the timing of the "Great Dying" that was characterized by large-scale depopulation which directly or indirectly favored forest expansion in the Americas (Koch et al., 2019). At the top of zone 3 (~1850–1950 CE), disturbance taxa increase at the expense of arboreal pollen, indicating renewed human activity that likely resulted in forest clearance from renewed farming, timbering, and other land use activities (Harvey et al., 2019). These anthropogenic disturbances were likely associated with land reclamation in the region after the independence of Guatemala from Spain.

6. Conclusions

Qualitative and quantitative analyses of palynomorph and elemental geochemistry data from the Punta Chapin core in Lake Izabal highlight the variability in the vegetation and environmental dynamics of the region during the last ~1300 calibrated years BP. Whereas pollen data provide an overview of the regional vegetation turnover, elemental geochemistry data offer information on soil erosion and moisture availability during the late Holocene. Under climate change scenarios, the survival of plants depends on their ability to adjust or migrate and acclimatize to new configurations of the bioclimatic space (Correa-Metrio et al., 2013). In the northern Neotropics, the last 1300 years have been characterized by multiple climatic events, such as the LIA and MCA with their associated changes in moisture availability, and the several droughts that typified the Terminal Classic Period (Gill et al., 2007; Kennett et al., 2012). The evidence from the Punta Chapin core indicates that, in the region, the most important ecological change within the last 1300 years was probably produced by changes in disturbance regimes that resulted from Maya presence and subsequent abandonment of the area. However, changes in moisture availability appear to have also played an important role in modulating vegetation composition and structure. These two factors, are clearly reflected by our pollen results. The celerity of vegetation turnover revealed by our record, together with the moister conditions that characterize LIB in the regional context (Duarte et al., 2021), highlight the potential of the region as a refugium for ecosystems in times of climatic turmoil. Our integrated analyses suggest combined anthropogenic influences and climatic forcing on the vegetational changes in the LIB during the Late Holocene. Anthropogenic influences appear as first-order controls on the variability of vegetation, whereas moisture availability and evaporation rates appear to have acted on a second-order scale.

Data availability

Data will be made available on request.

Declaration of Competing Interest

The authors of the manuscript titled "A millennium of anthropic and climatic dynamics in the Lake Izabal Basin, eastern lowland Guatemala" Erdoo Mongol, Francisca Oboh-Ikuenobe1, Jonathan Obrist-Farner, J. Enrique Moreno, and Alex Correa-Metrio declare no conflict of interest.

Acknowledgements

EM gratefully acknowledges the financial support of the following: the Nigerian Petroleum Technology Development Fund, two Geological Society of America Graduate Student Research Grants, National Association of Black Geoscientists Graduate Student Awards, and the Visiting Graduate Student Program of the National Lacustrine Core Facility and the Continental Scientific Drilling Coordination Office. E.M is also thankful to Dr. Carlos Jaramillo and Dr. Dena Smith-Nufio for their mentorship. We thank the anonymous reviewers for helping to improve the quality of the manuscript.

Appendix A. Supplementary data

Supplementary data to this article can be found online at https://doi.org/10.1016/j.revpalbo.2023.104872.

References

- Anchukaitis, K.J., Smerdon, J.E., 2022. Progress and uncertainties in global and hemispheric temperature reconstructions of the Common Era. Quat. Sci. Rev. 286, 107537.
- Bartole, R., Lodolo, E., Obrist-Farner, J., Morelli, D., 2019. Sedimentary architecture, structural setting, and Late Cenozoic depocentre migration of an asymmetric transtensional basin: Lake Izabal, eastern Guatemala. Tectonophysics 750, 419–433.
- Beach, T., Luzzadder-Beach, S., Dunning, N., Jones, J., Lohse, J., Guderjan, T., Bozarth, S., Millspaugh, S., Bhattacharya, T., 2009. A review of human and natural changes in Maya Lowland wetlands over the Holocene. Quat. Sci. Rev. 28 (17–18), 1710–1724.
- Bhattacharya, T., Chiang, J.C., Cheng, W., 2017. Ocean-atmosphere dynamics linked to 800–1050 CE drying in mesoamerica. Quat. Sci. Rev. 169, 263–277.
- Blaauw, M., Christen, J.A., 2011. Flexible paleoclimate age-depth models using an autoregressive gamma process. Bayesian Anal. 6, 457–474.
- Boyle, J.F., 2002. Inorganic geochemical methods in palaeolimnology. In: Last, W.M., Smol, J.P. (Eds.), Tracking Environmental Change Using Lake Sediments. Springer, Dordrecht, pp. 83–141.
- Brenner, M., Rosenmeier, M.F., Hodell, D.A., Curtis, J.H., 2002. Paleolimnology of the Maya lowlands: long-term perspectives on interactions among climate, environment, and humans. Anc. Mesoam. 13, 141–157.
- Brenner, M., Hodell, D.A., Curtis, J.H., Rosenmeier, M.F., Anselmetti, F.S., Ariztegui, D., 2003. Paleolimnological approaches for inferring past climate change in the Maya region: recent advances and methodological limitations. In: Gomez-Pompa, A., Allen, M.F., Fedick, S.L., Jiminez-Osornio, J.J. (Eds.), The Lowland Maya Area: Three Millennia at the Human-Wildland Interface. Haworth Press, Inc, New York, pp. 45–75.
- Brinson, M.M., Nordlie, F.G., 1975. II. Lakes. 8. Central and South America: Lake Izabal, Guatemala. SIL Proc. 1922–2010 19 (2), 1468–1479. https://doi.org/10.1080/03680770.1974.11896206.
- Bush, M.B., Weng, C., 2007. Introducing a new (freeware) tool for palynology. J. Biogeogr. 34, 377–380.
- Bush, M., Nascimento, M., Åkesson, C., Cárdenes-Sandí, G., Maezumi, S., Behling, H., Correa-Metrio, A., Church, W., Huisman, S., Kelly, T., 2021. Widespread reforestation before European influence on Amazonia. Science 372, 484–487.
- Caballero-Rodríguez, D., Lozano-García, S., Correa-Metrio, A., 2017. Vegetation assemblages of central Mexico through the late Quaternary: modern analogs and compositional turnover. J. Veg. Sci. 28, 504–514.
- Caballero-Rodríguez, D., Correa-Metrio, A., Lozano-García, S., Sosa-Nájera, S., Ortega, B., Sanchez-Dzib, Y., Aguirre-Navarro, K., Sandoval-Montaño, A., 2018. Late-Quaternary spatiotemporal dynamics of vegetation in central Mexico. Rev. Palaeobot. Palynol. 250, 44-52.
- Caffrey, M.A., Taylor, M.J., Sullivan, D.G., 2011. A 12,000-year record of vegetation and climate change from the Sierra de Los Cuchumatanes, Guatemala. J. Lat. Am. Geogr. 10, 129–151.
- Colinvaux, P.A., de Oliveira, P.E., Moreno, J.E., 1999. Amazon Pollen Manual and Atlas = Manual e Atlas Palinológico da Amazônia. Harwood Academia Press, Amsterdam, The Netherlands, p. 332.
- Correa-Metrio, A., Bush, M.B., Pérez, L., Schwalb, A., Cabrera, K.R., 2011. Pollen distribution along climatic and biogeographic gradients in northern central America. The Holocene 21, 681–692.
- Correa-Metrio, A., Bush, M.B., Hodell, D.A., Brenner, M., Escobar, J., Guilderson, T., 2012a. The influence of abrupt climate change on the ice-age vegetation of the central American lowlands. J. Biogeogr. 39, 497–509.
- Correa-Metrio, A., Bush, M.B., Cabrera, K.R., Sully, S., Brenner, M., Hodell, D.A., Escobar, J., Guilderson, T., 2012b. Rapid climate change and no-analog vegetation in lowland central America during the last 86,000 years. Quat. Sci. Rev. 38, 63–75.
- Correa-Metrio, A., Bush, M., Lozano-García, S., Sosa-Nájera, S., 2013. Millennial-scale temperature change velocity in the continental northern Neotropics. PLoS One 8 (12), e81958.
- Correa-Metrio, A., Meave, J.A., Lozano-García, S., Bush, M.B., 2014a. Environmental determinism and neutrality in vegetation at millennial time scales. J. Veg. Sci. 25, 627–635.
- Correa-Metrio, A., Dechnik, Y., Lozano-García, S., Caballero, M., 2014b. Detrended correspondence analysis: a useful tool to quantify ecological changes from fossil data sets. Bol. Soc. Geol. Mex. 66, 135–143.

- Correa-Metrio, A., Vélez, M.I., Escobar, J., St-Jacques, J.M., López-Pérez, M., Curtis, J., Cosford, J., 2016. Mid-elevation ecosystems of Panama: future uncertainties in light of past global climatic variability. J. Quat. Sci. 31, 731–740.
- Curtis, J.H., Hodell, D.A., Brenner, M., 1996. Climate variability on the Yucatan Peninsula (Mexico) during the past 3500 years, and implications for Maya cultural evolution. Ouat. Res. 46 (1), 37–47.
- Deevey, E.S., 1965. Sampling lake sediments by use of the Livingstone sampler. In: Kummel, B., Raup, D. (Eds.), Handbook of Paleontological Techniques. Freeman, San Francisco, pp. 521–529.
- Delcourt, H.R., Delcourt, P.A., 1991. Quaternary Ecology: A Paleoecological Perspective. Chapman & Hall, Cornwall, UK.
- Duarte, E., Obrist-Farner, J., Correa-Metrio, A., Steinman, B.A., 2021. A progressively wetter early through middle Holocene climate in the eastern lowlands of Guatemala. Earth Planet. Sci. Lett. 561, 116807.
- Dull, R.A., 2007. Evidence for forest clearance, agriculture, and human-induced erosion in Precolumbian El Salvador. Ann. Assoc. Am. Geogr. 97 (1), 127–141.
- Faegri, K., Iversen, J., Kaland, P.E., Krzywinski, K., 1989. Textbook of Pollen Analysis. Caldwell.
- Fisher, M.M., Brenner, M., Reddy, K.R., 1992. A simple, inexpensive piston corer for collecting undisturbed sediment/water interface profiles. J. Paleolimnol. 7, 157–161.
- Franco-Gaviria, F., Caballero-Rodríguez, D., Correa-Metrio, A., Pérez, L., Schwalb, A., Cohuo, S., Macario-González, L., 2018a. The human impact imprint on modern pollen spectra of the Maya Lands. Bol. Soc. Geol. Mex. 70, 61–78.
- Franco-Gaviria, F., Correa-Metrio, A., Cordero-Oviedo, C., López-Pérez, M., Cárdenes-Sandí, G.M., Romero, F.M., 2018b. Effects of late Holocene climate variability and anthropogenic stressors on the vegetation of the Maya highlands. Quat. Sci. Rev. 189, 76–90.
- genic stressors on the vegetation of the Maya nighlands. Quat. Sci. Rev. 189, 76–90. Gill, R.B., Mayewski, P.A., Nyberg, J., Haug, G.H., Peterson, L.C., 2007. Drought and the Maya collapse. Anc. Mesoam. 18 (2), 283–302.
- Giunta, G., Beccaluva, L., Coltorti, M., Cutrupia, D., Dengo, C., Harlow, G., Mota, B., Padoa, E., Rosenfeld, J., Siena, F., 2002. The Motagua Suture Zone in Guatemala, Field Trip Guide Book of the IGCP 433 Workshop and 2nd Italian–Latin American Geological Meeting in Memory of Gabriel Dengo. Ofioliti 27 (1), 47–72.
- Graham, A., 2010a. Late Cretaceous and Cenozoic History of Latin American Vegetation and Terrestrial Environments. Missouri Botanical Garden Press, p. 618.
- Graham, A., 2010b. A Natural History of the New World: The Ecology and Evolution of Plants in the Americas. University of Chicago Press, Chicago.
- Guderjan, T.H., Krause, S., 2011. Identifying the extent of ancient Maya ditched fields in the Río Hondo Valley of Belize and Mexico: a pilot study and some of its implications. Res. Rep. Belizean Archaeol. 8, 127–136.
- Harvey, W., Nogué, S., Stansell, N., Petrokofsky, G., Steinman, B., Willis, K.J., 2019. The legacy of Pre–Columbian fire on the pine–oak forests of Upland Guatemala. Front. Forests Global Change https://doi.org/10.3389/ffgc.2019.00034.
- Haug, G.H., Hughen, K.A., Sigman, D.M., Peterson, L.C., Röhl, U., 2001. Southward migration of the intertropical convergence zone through the Holocene. Science 293, 1304–1308.
- Hernández, E., Obrist-Farner, J., Brenner, M., Kenney, W.F., Curtis, J.H., Duarte, E., 2020. Natural and anthropogenic sources of lead, zinc, and nickel in sediments of Lake Izabal, Guatemala. J. Environ. Sci. 96, 117–126.
- Hodell, D.A., Curtis, J.H., Brenner, M., 1995. Possible role of climate in the collapse of Classic Maya civilization. Nature 375, 391.
- Hodell, D.A., Brenner, M., Curtis, J.H., Medina-Gonzalez, R., Can, E.I.C., Albornaz-Pat, A., Guilderson, T.P., 2005a. Climate change on the Yucatan Peninsula during the little ice age. Quat. Res. 63 (2), 109–121.
- Hodell, D.A., Brenner, M., Curtis, J.H., 2005b. Terminal Classic drought in the northern Maya lowlands inferred from multiple sediment cores in Lake Chichancanab (Mexico). Quat. Sci. Rev. 24 (12–13), 1413–1427.
- Holst, I., Moreno, J.E., Piperno, D.R., 2007. Identification of teosinte, maize, and *Tripsacum* in Mesoamerica by using pollen, starch grains, and phytoliths. Proc. Natl. Acad. Sci. 104. 17608–17613.
- Islebe, G.A., Hooghiemstra, H., 1995. Recent pollen spectra of highland Guatemala. J. Biogeogr. 22, 1091–1099.
- Islebe, G.A., Hooghiemstra, H., Brenner, M., Curtis, J.H., Hodell, D.A., 1996. A Holocene vegetation history from lowland Guatemala. The Holocene 6, 265–271.
- Jaramillo, C.A., Dilcher, D.L., 2001. Middle Paleogene palynology of central Colombia, South America: a study of pollen and spores from tropical latitudes. Palaeontogr. Abt. B Paläophytol. 258, 87–213.
- Jaramillo, C., Rueda, M., 2019. A Morphological Electronic Database of Cretaceous-Tertiary and Extant Pollen and Spores from Northern South America, v. 2019. Smithsonian Tropical Research Institute, Panama City, Panama. http://biogeodb.stri.si.edu/ jaramillosdb/web/morphological/.
- Jolliffe, I., 1986. Principal Component Analysis. 2nd edition. Springer-Verlag, New York, p. 487.
- Juggins, S., 2017. rioja: Analysis of Quaternary Science Data, R Package Version 0.9-21.
 Kennett, D.J., Breitenbach, S.F., Aquino, V.V., Asmerom, Y., Awe, J., Baldini, J.U., Bartlein, P.,
 Culleton, B.J., Ebert, C., Jazwa, C., Macri, M.J., 2012. Development and disintegration of
- Maya political systems in response to climate change. Science 338 (6108), 788–791. Koch, A., Brierley, C., Maslin, M.M., Lewis, S.L., 2019. Earth system impacts of the European arrival and Great Dying in the Americas after 1492. Quat. Sci. Rev. 207, 13–36.
- Krause, S., Beach, T.P., Luzzadder-Beach, S., Cook, D., Bozarth, S.R., Valdez Jr., F., Guderjan, T.H., 2021. Tropical wetland persistence through the Anthropocene: multiproxy reconstruction of environmental change in a Maya agroecosystem. Anthropocene 34, 100384
- Kylander, M.E., Ampel, L., Wohlfarth, B., Veres, D., 2011. High-resolution X-ray fluorescence core scanning analysis of Les Echets (France) sedimentary sequence: new insights from chemical proxies. J. Quat. Sci. 26, 109–117.

- Leonard, D., Sedov, S., Solleiro-Rebolledo, E., Fedick, S.L., Diaz, J., 2019. Ancient Mayan use of hidden soilscapes in the Yalahau wetlands, northern Quintana Roo, Mexico. Bol. Soc. Geol. Mex. 71, 93–119.
- Leyden, B.W., 1987. Man, and climate in the Maya lowlands. Quat. Res. 28 (3), 407–414.
 Leyden, B.W., 2002. Pollen evidence for climatic variability and cultural disturbance in the Maya lowlands. Anc. Mesoam. 13, 85–101.
- Lozano-García, M., Caballero, M., Ortega, B., Rodríguez, A., Sosa, S., 2007. Tracing the effects of the Little Ice Age in the tropical lowlands of eastern Mesoamerica. Proc. Natl. Acad. Sci. 104 (41), 16200–16203.

 Magaña, V., Amador, J.A., Medina, S., 1999. The midsummer drought over Mexico and
- Magaña, V., Amador, J.A., Medina, S., 1999. The midsummer drought over Mexico and central America. J. Clim. 12 (6), 1577–1588.
 Mann, M.E., Zhang, Z., Rutherford, S., Bradley, R.S., Hughes, M.K., Shindell, D., Ammann, C.,
- Mann, M.E., Zhang, Z., Rutherford, S., Bradley, R.S., Hughes, M.K., Shindell, D., Ammann, C., Faluvegi, G., Ni, F., 2009. Global signatures and dynamical origins of the Little Ice Age and Medieval Climate Anomaly. Science 326 (5957), 1256–1260.
- Marchant, R., Almeida, L., Behling, H., Berrio, J.C., Bush, M., Cleef, A., Duivenvoorden, J., Kappelle, M., de Oliveira, P., de Oliveira-Filho, A.T., Lozano-Garcia, S., Hooghiemstra, H., Ledru, M.-P., Ludlow-Wiechers, B., Markgraf, V., Mancini, V., Paez, M., Preto, A., Rangel, O., Salgado-Labouriau, M.L., 2002. Distribution and ecology of parent taxa of pollen lodged within the Latin American Pollen Database. Rev. Palaeobot. Palynol. 121. 1–75.
- Martinez, C., Goddard, L., Kushnir, Y., Ting, M., 2019. Seasonal climatology and dynamical mechanisms of rainfall in the Caribbean. Clim. Dyn. 53 (1), 825–846.
- McGregor, H.V., Evans, M.N., Goosse, H., Leduc, G., Martrat, B., Addison, J.A., Mortyn, P.G., Oppo, D.W., Seidenkrantz, M.-S., Sicre, M.-A., 2015. Robust global ocean cooling trend for the pre-industrial Common Era. Nat. Geosci. 8, 671–677.
- Medina-Elizalde, M., Burns, S.J., Lea, D.W., Asmerom, Y., von Gunten, L., Polyak, V., Vuille, M., Karmalkar, A., 2010. High resolution stalagmite climate record from the Yucatán Peninsula spanning the Maya terminal classic period. Earth Planet. Sci. Lett. 298 (1–2), 255–262.
- Meyers, P.A., 1997. Organic geochemical proxies of paleoceanographic, paleolimnologic, and paleoclimatic processes. Org. Geochem. 27, 213–250.
- Meyers, P.A., 2003. Applications of organic geochemistry to paleolimnological reconstructions: a summary of examples from the Laurentian Great Lakes. Org. Geochem. 34, 261–289.
- Moreno, J.E., Vergara, D., Jaramillo, C., 2014. Las colecciones palinológicas del Instituto Smithsonian de Investigaciones Tropicales (STRI), Panamá. Boletín de la Asociación Latinoamericana de Paleobotánica y Palinología (ALPP) 14, 207–222.
- Mueller, A.D., Islebe, G.A., Hillesheim, M.B., Grzesik, D.A., Anselmetti, F.S., Ariztegui, D., Brenner, M., Curtis, J.H., Hodell, D.A., Venz, K.A., 2009. Climate drying and associated forest decline in the lowlands of northern Guatemala during the late Holocene. Quat. Res. 71, 133–141.
- Mueller, A.D., Islebe, G.A., Anselmetti, F.S., Ariztegui, D., Brenner, M., Hodell, D.A., Hajdas, I., Hamann, Y., Haug, G.H., Kennett, D.J., 2010. Recovery of the forest ecosystem in the tropical lowlands of northern Guatemala after disintegration of Classic Maya polities. Geology 38, 523–526.
- Nixon, K.C., 2006. Global and neotropical distribution and diversity of oak (genus *Quercus*) and oak forests. In: Kapppelle, M. (Ed.), Ecology and Conservation of Neotropical Montane Oak Forests. Springer, Berlin Heidelberg, pp. 4–13.
- Nooren, K., Hoek, W.Z., Dermody, B.J., Galop, D., Metcalfe, S., Islebe, G., Middelkoop, H., 2018. Climate impact on the development of Pre-Classic Maya Civilisation. Clim. Past 14, 1253–1273.
- Obrist-Farner, J., Brenner, M., Curtis, J.H., Kenney, W.F., Salvinelli, C., 2019. Recent onset of eutrophication in Lake Izabal, the largest water body in Guatemala. J. Paleolimnol. 62, 250, 272
- Obrist-Farner, J., Eckert, A., Locmelis, M., Crowley, J.L., Mota-Vidaure, B., Lodolo, E., Rosenfeld, J., Duarte, E., 2020. The role of the Polochic Fault as part of the North

- American and Caribbean Plate boundary: insights from the infill of the Lake Izabal Basin. Basin Res. 32 (6), 1347–1364.
- Obrist-Farner, J., Brenner, M., Stone, J.R., Wojewódka-Przybył, M., Bauersachs, T., Eckert, A., Locmelis, M., Curtis, J.H., Zimmerman, S.R., Correa-Metrio, A., Schwark, L., 2022a. New estimates of the magnitude of the sea-level jump during the 8.2 ka event. Geology 50 (1), 86–90.
- Obrist-Farner, J., Steinman, B.A., Stansell, N.D., Maurer, J., 2022b. Incoherency in Central American Hydroclimate Proxy Records Spanning the Last Millennium. Authorea Preprints.
- Oksanen, J., Blanchet, G., Friendly, M., Kindt, R., Legendre, P., McGlin, D., Minchin, P., O'Hara, B., Simpson, G.L., Solymos, P., Stevens, M.H.H., Szoecs, E., Wagner, H., 2020. vegan: Community Ecology Package, 2.5-7 ed The R Project for Statistical Computing.
- Punt, W., Hoen, P.P., Blackmore, S., Nilsson, S., Le Thomas, A., 2007. Glossary of pollen and spore terminology. Rev. Palaeobot, Palynol. 143, 1–81.
- R Core Team, 2021. R. A Language and Environment for Statistical Computing. R Foundation for Statistical Computing, Vienna, Austria See https://www.R-project.org.
- Reimer, P.J., 2020. Composition and consequences of the IntCal20 radiocarbon calibration curve, Ouat. Res. 96, 22–27.
- Richardson, D.M., 1998. Ecology and Biogeography of Pinus. Cambridge University Press, Cambridge, UK.
- Roubik, D.W., Moreno, J.E., 1991. Pollen and spores of Barro Colorado Island. Monographs in Systematic Botany. 36. Missouri Botanical Garden, p. 268.
- Rull, V., 2009. Microrefugia. J. Biogeogr. 36 (3), 481-484.
- Rzedowski, J., 2006. Vegetación de México, 1ra. Edición digital ed. Comisión Nacional para el Conocimiento y Uso de la Biodiversidad. México D.F. p. 504.
- Standley, P.C., Steyermark, J.A., 1945. The Vegetation of Guatemala, A Brief Review. Plants and Plant Sciences in Latin America. Chronica Botanica Co, Waltham, Mass, pp. 275–278.
- Steinman, B.A., Stansell, N.D., Mann, M.E., Cooke, C.A., Abbott, M.B., Vuille, M., Bird, B.W., Lachniet, M.S., Fernandez, A., 2022. Interhemispheric antiphasing of neotropical precipitation during the past millennium. Proc. Natl. Acad. Sci. 119 (17), e2120015119. Steyermark, J.A., 1950. Flora of Guatemala. Ecology 31, 368–372.
- Tropicos.org, 2020. Missouri Botanical Garden. Accessed 08 Nov 2020 http://www.tropicos.org.
- Turner, B.L., Sabloff, J.A., 2012. Classic Period collapse of the Central Maya Lowlands: insights about human–environment relationships for sustainability. Proc. Natl. Acad. Sci. 109 (35), 13908–13914.
- Vinson, G.L., 1962. Upper Cretaceous and tertiary stratigraphy of Guatemala. AAPG Bull. 46 (4), 425–456.
- Wahl, D., Schreiner, T., Byrne, R., Hansen, R., 2007a. A paleoecological record from a Late Classic Maya reservoir in the north Petén. Lat. Am. Antiq. 18 (2), 212–222.
- Wahl, D., Byrne, R., Schreiner, T., Hansen, R., 2007b. Palaeolimnological evidence of late-Holocene settlement and abandonment in the Mirador Basin, Peten, Guatemala. The Holocene 17 (6), 813–820.
- Wahl, D., Hansen, R.D., Byrne, R., Anderson, L., Schreiner, T., 2016. Holocene climate variability and anthropogenic impacts from Lago Paixban, a perennial wetland in Péten, Guatemala. Glob. Planet. Chang. 138, 70–81.
- White, D.A., Hood, C.S., 2004. Vegetation patterns and environmental gradients in tropical dry forests of the northern Yucatan Peninsula. J. Veg. Sci. 15 (2), 151–160.
- Whitney, B.S., Rushton, E.A., Carson, J.F., Iriarte, J., Mayle, F.E., 2012. An improved methodology for the recovery of *Zea mays* and other large crop pollen, with implications for environmental archaeology in the Neotropics. The Holocene 22, 1087–1096.
- Wilson, H.H., 1974. Cretaceous sedimentation and orogeny in nuclear Central America. Am. Assoc. Pet. Geol. Bull. 58, 1348–1396.